

Short Term Wave Energy Variability off the West Coast of Ireland

G. Nolan¹, J.V. Ringwood² and B. Holmes³

¹ EirGrid Plc.

27 Lower Fitzwilliam Street, Dublin 2, Ireland
E-mail: gary.nolan@eirgrid.com

² Department of Electronic Engineering, National University of Ireland Maynooth,
Maynooth, Co. Kildare, Ireland

E-mail: john.ringwood@eeng.nuim.ie

³Hydraulics and Maritime Research Centre,
University College Cork,
Cork, Ireland

E-mail: hmrc@ucc.ie

Abstract

Within the context of wave energy conversion, this paper investigates the practice of using wave (frequency) spectra to characterise wind waves. In particular, this paper looks at the major shortfall of the wave spectrum - its lack of information provision on the temporal variability of the wave activity. Finally, the issue of different spectral shapes with the same seaway summary statistics (i.e. H_s , the significant wave height, and T_z , the mean zero crossing wave period) is investigated. Measured wave data recorded off the West Coast of Ireland provides the basis for this analysis, with the wavelet transform providing the primary analysis tool.

Keywords: Energy variability, wave spectra, wavelet transform, double-peaked spectra

Introduction

The characteristics of wind generated waves observed in the ocean varies somewhat randomly with time, with both wave period and wave height varying from one cycle to another. Consequently, the true characteristics of a wave profile can only be achieved through stochastic analysis. One of the most useful parameterisations of a wave profile is the wave spectral density function (often simply called the wave spectrum), $S(\omega)$, which details the energy per unit area of wave surface for each wave component of the total wave system (sample wave spectrum illustrated in Fig. 1). Useful information, such as the wave frequency corresponding to the peak (predominant) frequency, can be ascertained from the wave spectrum. Some useful statistical results can also be calculated from the moments of the wave

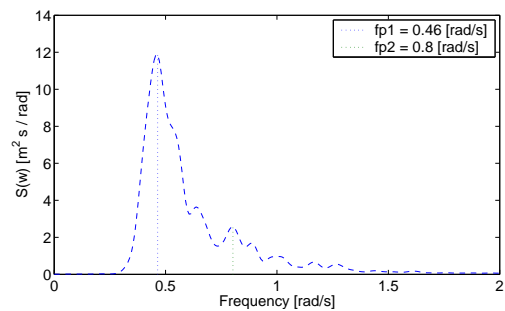


Figure 1: Sample wave spectrum, $S(\omega)$

spectrum. The n^{th} spectral moment is defined as:

$$m_n = \int_0^{\infty} \omega^n S(\omega) d\omega \quad (1)$$

with the zero order moment given as:

$$m_0 = \int_0^{\infty} S(\omega) d\omega \quad (2)$$

m_0 is in fact equal to the total variance of the sea surface elevation with $\rho g m_0$ equal to the total wave energy (per unit area), where ρ is the water density. In terms of spectral moments, the significant wave height (defined as the mean of the one third highest waves) is given by:

$$H_s = 4\sqrt{m_0} \quad (3)$$

while the zero mean crossing period is defined as:

$$T_z = \sqrt{\frac{m_0}{m_2}} \quad (4)$$

does not give any indication of the temporal variability of energy within the wave profile and, more importantly, the temporal variability of the distribution of energy with frequency. No information relative to important questions (for wave energy device designers) such as ‘does the peak frequency remain relatively constant across the wave profile?’ can be obtained from the wave spectrum. For example, is it reasonable to assume that, across the wave record which produced the wave spectrum in Fig. 1 optimal energy absorption by a wave energy converter (WEC) is achieved when the WEC is tuned to the peak frequency (in monochromatic waves maximum energy absorption is achieved when the natural frequency of the WEC is equal to the incident wave frequency [1]) or does the WEC need to actively track different frequencies across the wave record? It is this lack of information about the temporal variability of the wave activity that is causing, in some fields, the use of the wave spectrum to be questioned [2]. Not least in the emerging field of wave energy extraction is accurate temporal, as well as spectral, information required.

The study presented in this paper is based on analysis of recorded single point sea surface elevation data. The measured data was recorded off the West Coast of Ireland at 52° 39’ N, 9° 47’ W. The data consists of complete sets of 20 minute records recorded once every hour, with a sampling period of 0.39 seconds, for the months of Dec 2003, May 2004, and from October 2004 through to March 2005. A 20-minute time series of single point sea surface elevation data is for the purpose of this study referred to as a single wave record.

1 Obtaining Time-Frequency Information

1.1 The Short Term Fourier Transform

A simple and intuitive solution to obtaining both frequency and time domain information from a time series consists of pre-windowing the series around a particular time point, calculating its Fourier transform, and repeating this at regular time intervals across the series. This practice is known as the short-term Fourier transform (STFT) or as the windowed Fourier transform and gives time local information by calculating spectra of local sections of the time series. The narrower the window used, the better the time resolution, but the frequency resolution becomes poorer (and vice versa). When analysing the measured wave record data, the STFT is appropriate for assessing the wave activity over a number of hours or a single day. Fig. 2 illustrates a sample STFT. The Fourier transform of each hourly 20 minute section of data recorded on February 12th has been calculated and plotted consecutively.

To assess the variability of wave activity over shorter periods, such as minutes, the use of the STFT is no longer appropriate as extremely poor frequency resolution is obtained when achieving such time resolution. Unlike the STFT, the *Wavelet Transform* allows accurate localisation both in the time and frequency domain.

1.2 The Wavelet Transform

Whereas the Fourier transform breaks a signal into a series of sine waves of different frequencies, the wavelet transform utilises *wavelets* as basic functions, which are scaled and shifted versions of the so called *mother wavelet* [3]. The wavelet transform allows localisation in the time domain via translations of the wavelet, and in the frequency domain via dilations of the wavelet. The mother wavelet is itself of finite length (compact support) and typically a fast decaying oscillating waveform. In

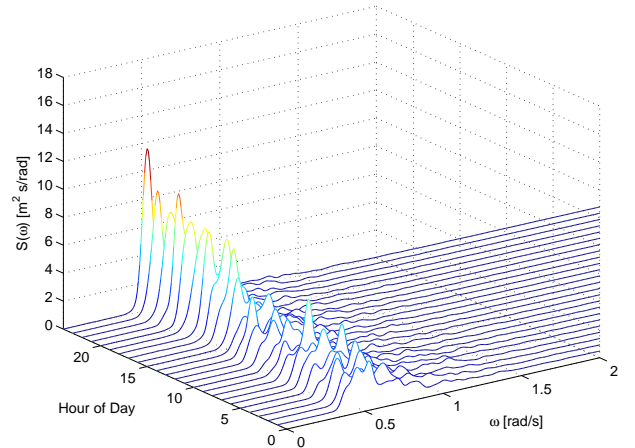


Figure 2: Sample STFT

general, the wavelet transform of the signal $x(t)$ is defined as:

$$WT(b, \tau) = \langle x, \psi_{b, \tau} \rangle = \int_{-\infty}^{\infty} x(t) \psi_{b, \tau}(t) dt \quad (5)$$

with the set of continuously translated and dilated wavelets being generated from the mother wavelet ψ as:

$$\psi_{b, \tau}(t) = \frac{1}{\sqrt{b}} \psi \left(\frac{t - \tau}{b} \right) \quad (6)$$

where τ is the translation parameter, relating to the location of the wavelet function, ψ , as it is shifted through the signal, and b is the scale dilation parameter. Large scales (for detecting low frequency components) dilate the signal, while small scales (for detecting high frequency components) compress the signal. Notice that the wavelet transform merely performs the convolution operation of the signal and the basis function. The wavelet coefficients, $WT(b, \tau)$, effectively represent the correlation between the current wavelet and a localised section of the signal. If the signal has a major component of the frequency corresponding to the given scale, then the wavelet at this scale is close to the signal at that particular location and the corresponding wavelet transform coefficient, determined at this point, has a relatively large value [3]. For a more rigorous introduction to the wavelet transform the reader should consider [4, 5].

One of the most extensively used mother wavelets is the Morlet wavelet:

$$\psi(t) = \cos(\omega_0 t) e^{-\frac{t^2}{2\sigma^2}} \quad (7)$$

There are many different families of mother wavelets each with a specific utility for different applications. The Morlet wavelet, as described in eq. (7), and illustrated in Fig. 3, is an appropriate mother wavelet for time-frequency analysis.

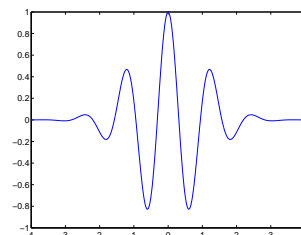


Figure 3: Morlet wavelet

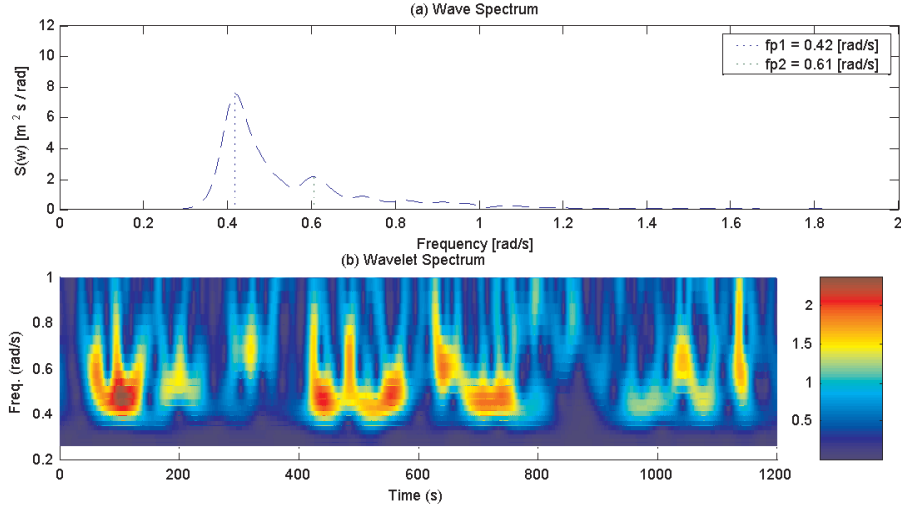


Figure 4: Sample wave spectrum and corresponding wavelet transform

Fig. 4 presents an example illustrating the wave (Fourier) spectrum and wavelet spectrum calculated from a wave record recorded on the 11th of February 2005. The wave spectrum is given in (a) while (b) shows the corresponding wavelet spectrum. The wavelet spectrum is illustrated as energy density contours in the two dimensional time-frequency space (time on the horizontal axis and frequency on the vertical axis). Notice that the wavelet spectrum clearly shows the intermittency of the wave activity. Both the magnitude and the distribution with frequency of the wave energy is clearly not constant across the original wave record, as is suggested from the wave spectrum in part (a).

2 Analysis

This section of the paper uses the measured wave record data to investigate:

- The short term variability of the peak frequency (one of the most important parameters for wave energy conversion),
- The issue of different spectral shapes having the same sea-way summary statistics (H_s and T_z), and
- The practice of simulating the surface elevation of an ocean wave from a wave spectrum.

2.1 Short Term Variability of the Peak Frequency

Figure 5 illustrates the wave spectrum and wavelet spectrum of two wave records (referred to as time series A and B). Considering the changes over time in the distribution of energy with frequency in the wavelet spectrum of time series A (Fig. 5 (b)), it is seen that while the wave activity is clearly intermittent, the peak frequency remains relatively constant across the time series. In stark contrast, the wavelet spectrum of time series B (Fig. 5 (d)) shows a significant amount of variation in the peak frequency with time. Clearly, it is far more straightforward for a WEC to absorb the energy in the waves of time series A as there is a clear, and constant, peak frequency which the WEC can be tuned to.

An appropriate measure of the variability of the peak frequency with time is the weighted standard deviation of the peak frequency in the wavelet spectrum. Amplitude weighting is used

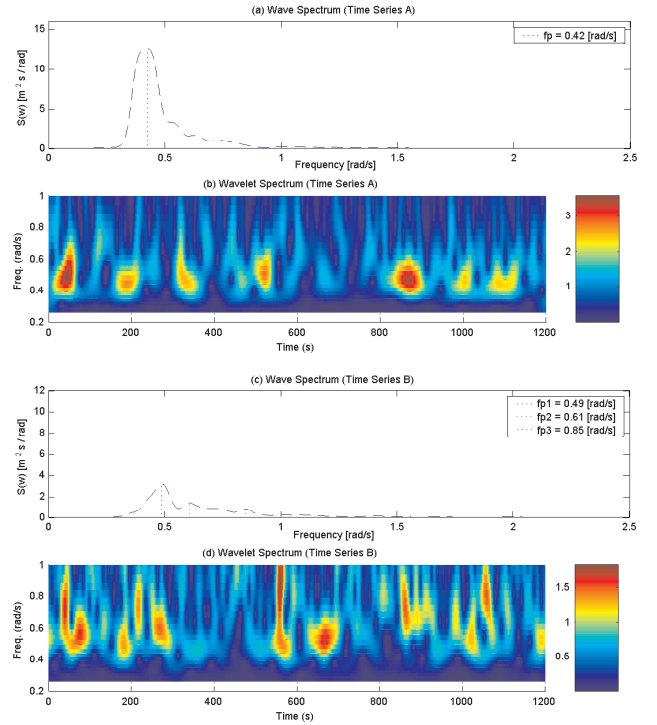


Figure 5: Wavelet spectrums illustrating different levels of peak frequency temporal variability

as the occasions of high amplitude (\equiv high energy) are of more importance to wave energy conversion than the times of low amplitude. Utilising the peak frequency at every time point in the wavelet spectrum the weighted standard deviation of the peak frequency, σ_w , is given by:

$$\sigma_w = \sqrt{\frac{\sum_{i=1}^{N'} w_i (x_i - \mu_w)^2}{(N' - 1) \sum_{i=1}^{N'} w_i}} \quad (8)$$

where w_i is the weight (amplitude) for the i th observation (peak frequency), N' is the number of non-zero weights, N is the

number of observations, and μ_w is the weighted mean peak frequency given by:

$$\mu_w = \frac{\sum_{i=1}^N w_i x_i}{N'} \quad (9)$$

For the wavelet spectrum of time series A (Fig. 5 (b)), $\sigma_w = 0.086$ rad/s and $\mu_w = 0.469$ rad/sec with $\sigma_w = 0.149$ rad/s and $\mu_w = 0.589$ rad/sec for the wavelet spectrum of time series B (Fig. 5 (d)).

Returning to the wave spectrum of Fig. 4 (a), two distinct peaks, as a result of the coexistence of two separate wave systems, can be observed in the spectrum. As is quite often the case on the West Coast of Ireland, waves consist of swell and local wind-generated waves. In the case of the West Coast of Ireland, the incident swell waves have been generated over the Atlantic Ocean and are quite often of large magnitude, since the fetch (the distance over which the waves develop) and the duration for which the wind blows are sufficient for the waves to achieve their maximum energy for a given wind speed (i.e. *fully developed waves*). In Fig. 4 (a), the large lower frequency peak is a result of the swell waves with the higher frequency peak attributed to the local wind generated waves. It is thought that over the course of the development of swell waves, short waves get overtaken by larger waves resulting in a train of more *regular long* waves (favourable waves for absorbing energy from) moving in a single direction [6]. This is most likely what is being seen in Fig. 5 (a) and (b), with a large regular swell system providing the relatively constant, in terms of peak frequency, wave conditions (note that the occurrence of wave grouping is still identifiable). In conclusion, on the West Coast of Ireland the wave systems consisting of mainly larger magnitude swell waves should be more regular than wave systems consisting of predominantly lower magnitude local wind waves. Hence, in the recorded wave data there should exist some level of inverse correlation between energy and variability. Again, if this were found to be true, it would be a favourable scenario for wave energy conversion.

In the left column of Fig. 6, the measure of peak frequency variability, σ_w , is plotted against the total wave energy per unit area (as described in the Introduction) for each wave record. Each row of the figure illustrates the results for the different months studied (as indicated by the title of each plot). In the right column of the same figure, μ_w is plotted against the total wave energy per unit area.

Using the information in the left column of the figure it is difficult to see any inverse correlation between energy and variability in the wave records. In most months, the mean σ_w appears to remain relatively constant across the range of wave energy values. As expected, an inverse correlation between energy and μ_w can be clearly seen in a number of months, with high energy wave systems (containing large swell waves) typically having a low μ_w . As mentioned previously, this is a result of the swell waves consisting of more regular *long* waves [6]. Table 1 details the average σ_w and μ_w for each of the studied months. Again, the higher energy winter months (especially December and January) demonstrate a lower mean μ_w than the other months (more long swell waves).

2.2 Different Spectral Shapes with the Same Summary Statistics

Figs. 7 and 8 illustrate examples of different spectral shapes with the same seaway summary statistics. By summary statistics it is meant H_s and T_z , the most commonly used parameters to characterise a sea state. Fig. 7 for example, illustrates two wave

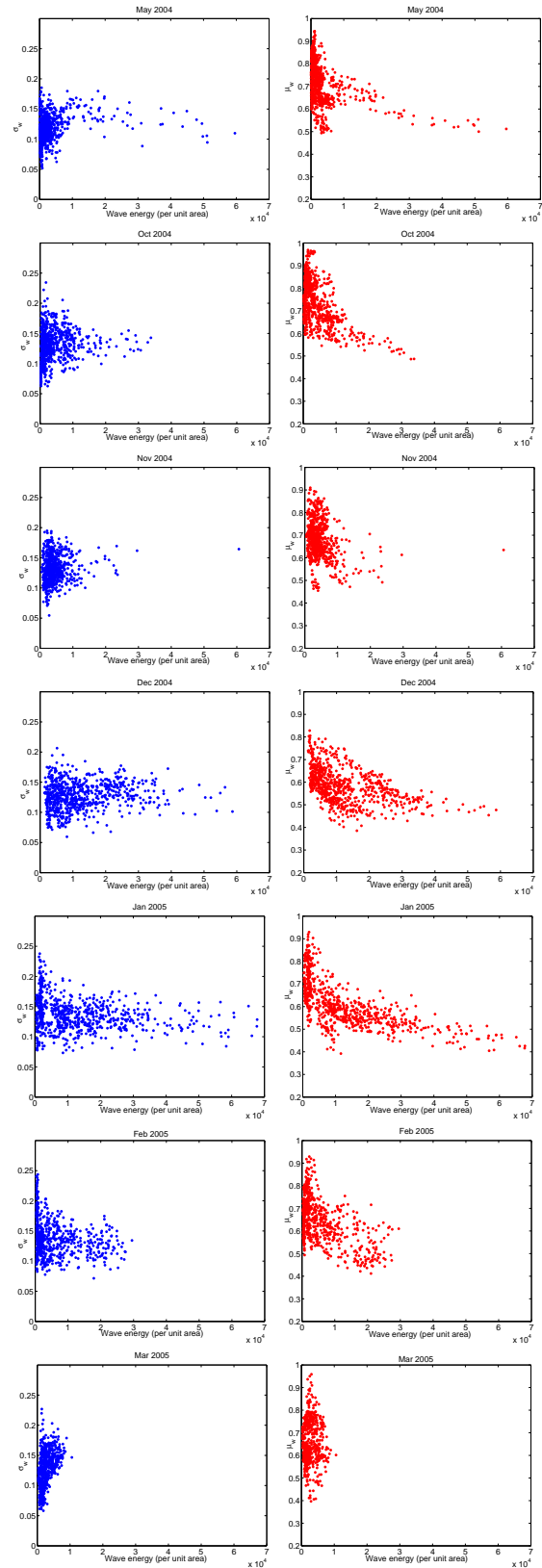


Figure 6: Energy plotted against the wavelet summary statistics

spectra obtained from two wave records recorded in December 2003. For each of the wave records, H_s and T_z are calculated

Month	Average	
	σ_w	μ_w
May 04	0.118	0.710
Oct 04	0.131	0.740
Nov 04	0.0.132	0.682
Dec 04	0.128	0.586
Jan 05	0.137	0.605
Feb 05	0.139	0.645
Mar 05	0.127	0.647

Table 1: Wavelet transform summary statistics

to be roughly 3 meters and 6 seconds respectively. Also illustrated in Fig. 7 is the Pierson Moskowitz spectral model [7] for $H_s = 3m$ and $T_z = 6s$. It is clear to see that while the three spectra have the same H_s and T_z , both the peak frequency and the distribution of energy with frequency is distinctly different for each of the spectra. Fig. 8 shows another set of spectra illustrating the same issue.

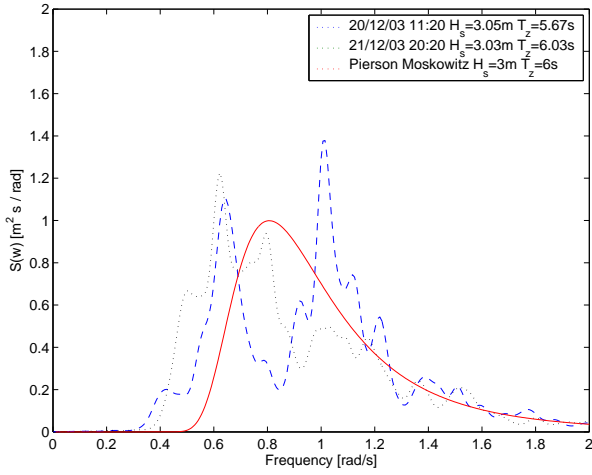


Figure 7: Different spectral shapes with the same summary statistics (example 1)

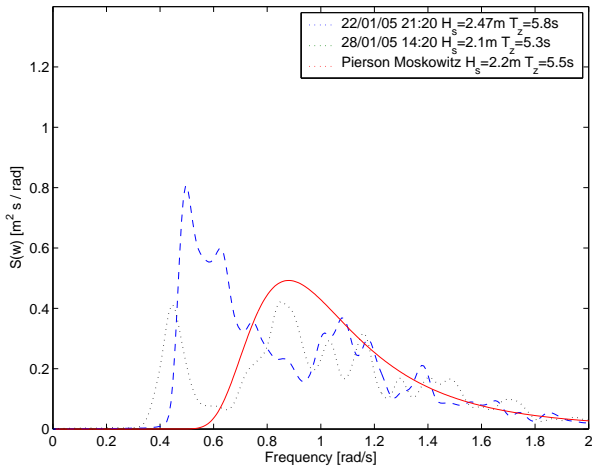


Figure 8: Different spectral shapes with the same summary statistics (example 2)

The reason these different spectral shapes have the same summary statistics is because the wave records associated with these spectra have the same variance (same total energy in the wave record, same area under the wave spectrum) and the parameters H_s and T_z are directly related to these (equations (3) and (4)).

From the recorded wave data, it appears that, more often than not, the wave spectrum obtained from the measured data differs in shape to the classic spectral shape (e.g. Pierson Moskowitz spectrum in Fig. 7) when coexisting wave systems (local wind waves and swell waves) are present i.e. when double peaked spectra are obtained.

This issue of misrepresentation of double peaked spectra, through the sole use of H_s and T_z brings into question the reliability of H_s and T_z as useful parameters within a wave energy conversion context. Currently H_s and T_z , with spectral models, are used in the form of joint distribution tables to give long term (possibly over a year) sea descriptions that are used in the design of WECs (in terms of designing parameters such as the WEC mass) and the design of WEC control systems. These long term descriptions are also used to give predictions of likely energy production from a WEC. Not only is the misrepresentation of double-peaked spectra an issue, the wave systems with double peaked spectra directly present a significant challenge to the WEC designer and control engineer alike.

To assess the significance of the problems associated with double-peaked spectra (and their potential misrepresentation) it is important to know the probability of occurrence of these spectra. Cummings et al. [8] determined that 25% of the wave spectra calculated using hindcast data from the North Atlantic were double peaked, while Guedes Soares and Nolasco [9] determined a range of 23-26% for data recorded off the coast of Portugal. It can be difficult to identify if the peaks in a wave spectrum correspond to the coexistence of different wave systems or if they are the result of the irregularity of the spectral estimates [10]. In many cases, the case is absolutely clear by visual inspection. However, to investigate the probability of occurrence of double peaked spectra in the data recorded off the West Coast of Ireland, a formal criterion is necessary. This criterion provides a definition for identification of double-peaked spectra and allows the task of their identification to be made automatically through a computer algorithm. The criterion used is one of the criteria detailed in Guedes Soares et al. [9] and is based on the use of confidence intervals. Details of the statistical variability of wave spectral estimates and the use and calculation of confidence intervals for wave spectral estimates can be found in [10, 11]. The confidence intervals for the spectral estimates with ν degrees of freedom (dependant on level of smoothing or averaging used in obtaining the spectrum) are given in terms of the chi-squared probability distribution as [11, 12]:

$$\left[\frac{\nu}{\chi^2_{\nu, \alpha/2}} \right] \hat{S}(\omega) \leq S(\omega) \leq \left[\frac{\nu}{\chi^2_{\nu, 1-\alpha/2}} \right] \hat{S}(\omega) \quad (10)$$

where α is the significance level, which is 0.1 for a 90% confidence interval, χ^2 is the critical value of the chi-square distribution for ν and α , $\hat{S}(\omega)$ is the estimated spectrum and $S(\omega)$ is the unknown true spectrum.

The following three conditions define the criterion for determining whether a spectrum is double-peaked (Fig. 9 is provided to aid the comprehension of the criterion):

1. The lower limit of the 90% confidence interval of the largest peak (point 1 in Fig. 9) must be higher than the adjacent minimum of the upper 90% confidence interval (point 2).

2. The minimum between the two peaks (point 3) should be below the lower 90% confidence interval of the smaller of the two peaks (point 4).
3. The lower peak (point 5) must be larger than 15% of the dominant peak (point 6).

The last condition of the criterion is included to overcome the noise level in the spectral estimate. However, it is noted that the value of 15% adopted by the developers of the criterion is largely arbitrary and based on judgement [9].

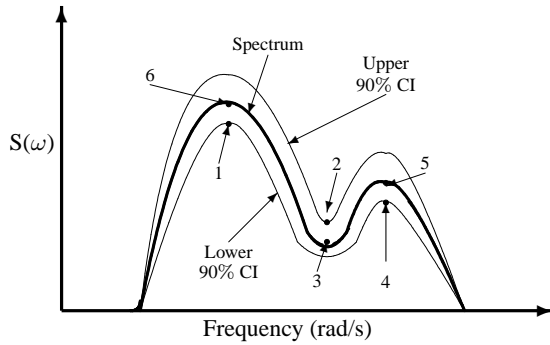


Figure 9: Criteria points used to identify double peaked spectra

Fig. 10 illustrates an example of the criterion in operation. The peaks attributed to different wave systems are highlighted by the red stars. Note that the peak at 0.72 rad/s is not identified as corresponding to an individual wave system, as it does not pass condition 2 of the criterion, yet the peak at 0.96 rad/s is.

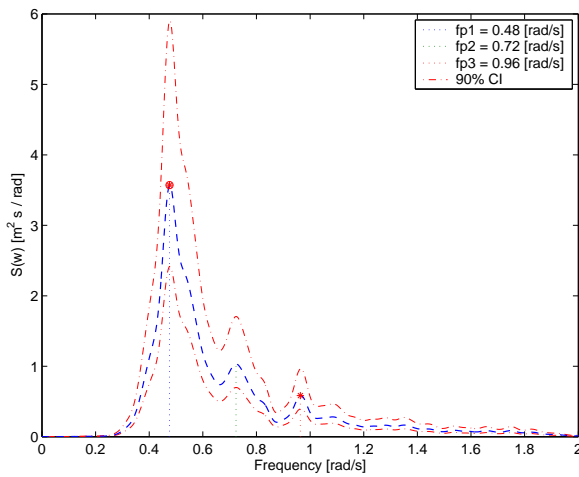


Figure 10: Example spectrum with two coexisting wave systems

Fig. 11 illustrates the results of applying the criterion to the all the wave records measured during the months January and March of 2005 (Fig. 11 (a) and (b) respectively). For further insight, the results are separated and displayed according to the total energy (per unit area) of the wave record.

It is difficult to estimate the percentage occurrence of double peaked spectra across a year, and to compare with the results of Cummings et al. [8], as it is clear that the level of occurrence varies highly across the year and this study does not have access to a full year of wave records.

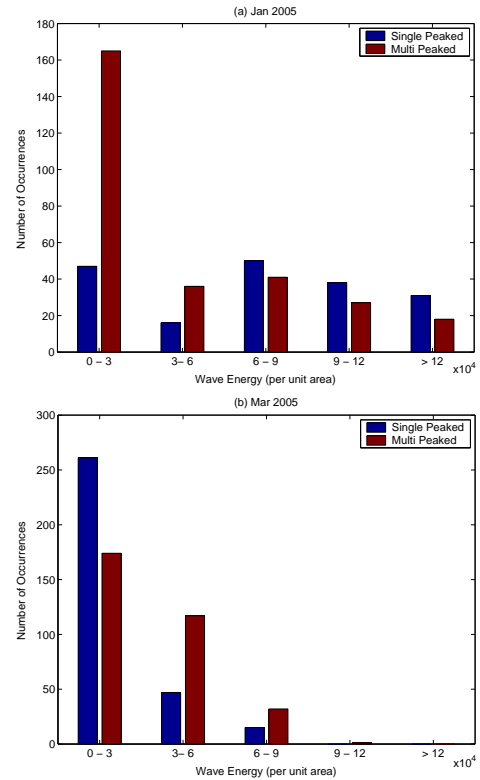


Figure 11: Occurrences of double and single peaked spectra broken down and displayed according to the total energy of the wave record

The criterion detailed and used above was developed to detect the coexistence of separate wave systems. Fig. 12 illustrates another spectrum deemed to have two coexisting wave systems. Considering this in a wave energy conversion context, the minor peak is so small in comparison to the dominant peak that it is essentially negligible. The local wind wave system (corresponding to the minor peak) is not significant enough to give any significantly misleading summary statistics (H_s and T_z).

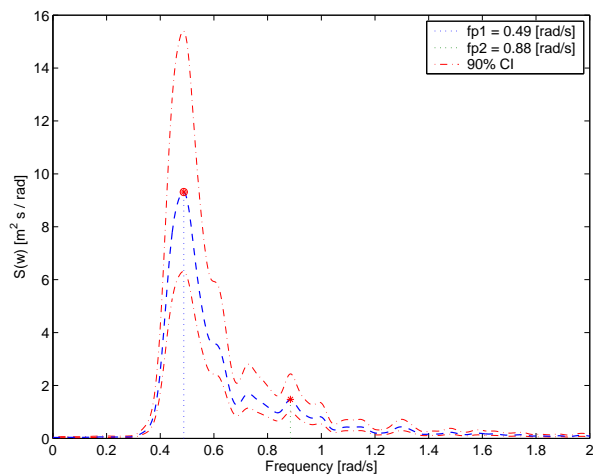


Figure 12: Second example of a spectrum with two coexisting wave systems

In an attempt to assess the number of wave records which

consist of two significant wave systems (i.e. the second peak is significant enough to result in a misleading summary statistic), the third condition of the detection criterion is altered such that the lower peak (point 5 in Fig. 9) must be larger than 50% of the dominant peak (point 6) for it to be considered as corresponding to a significant coexisting wave system. This value of 50% is chosen arbitrarily but is envisaged that this is an appropriate value to detect if the minor wave system is significant enough that the summary statistics for the wave record, and assuming a classical spectrum shape, will be significantly misleading to the shape of the calculated wave spectrum. Fig. 13 illustrates a spectrum deemed to consist of two significant wave systems using the amended criteria.

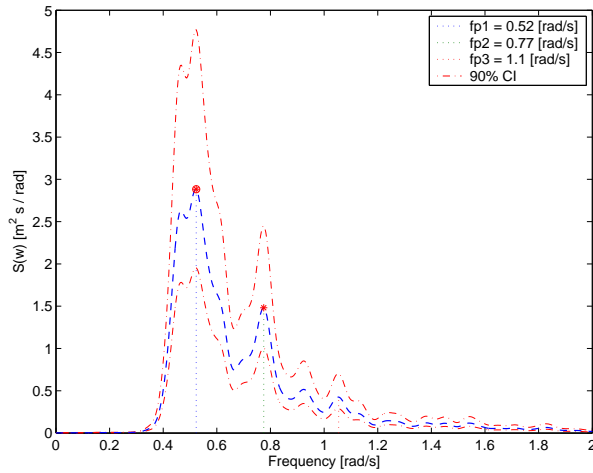


Figure 13: Spectrum with two *significant* wave systems

Fig. 14 illustrates the results of applying the amended criterion to the wave records measured during the months January and March of 2005 (Fig. 14 (a) and (b) respectively). Again, the results are separated and displayed according to the total energy (per unit area) of the wave record. Considering the information in Fig. 14, the following points are noteworthy:

- For wave records containing high energy wave systems almost all the spectra are identified as having a single significant peak (most likely a large dominant swell wave system).
- Most of the wave records identified as containing spectra with two significant wave systems occurred in the month of January on occasions when the total energy of the wave system is low (likely that the swell component is low and both the swell and local wind waves are detectable as significant coexisting wave systems).
- The quantity of wave records with high energy wave systems is significantly higher in January than March (as to be expected).

In conclusion, the occurrence of wave spectra containing two significant wave systems (significant enough that the spectrum is significantly misrepresented by its summary statistics and assuming a spectral model) is significantly lower than the occurrence of wave spectra containing two coexisting wave systems (estimated at 25% for the North Atlantic by Cummings et al. [8]) as per the criteria developed by Guedes Soares et al [9]. While the occurrence of wave records containing two significant wave systems may be low, when they do occur a problem can be found with the inaccurate use of the summary statistics

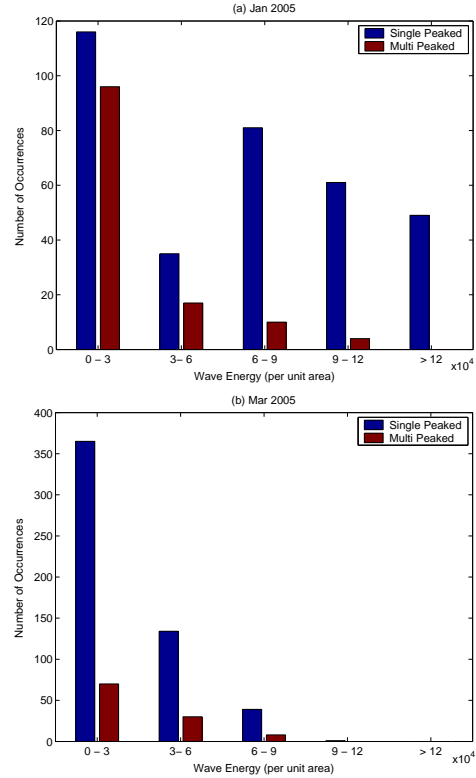


Figure 14: Occurrences of double and single peaked spectra (amended criteria) broken down and displayed according to the total energy of the wave record

H_s and T_z with a spectral model. However, further comfort can be taken from the fact that a large percentage of the wave records containing two significant wave systems occurred when the total energy of the wave systems was low and hence are not occasions of utmost importance for wave energy conversion.

2.3 Simulating Wave Records Using Spectral Models

This section uses the wavelet transform to look at the practice of using spectral models, such as the Pierson Moskowitz [7] or JONSWAP [13] spectra, to simulate realistic surface elevation wave records.

The surface elevation time series of a real ocean sea can be given by the superposition of a large number of regular wave components, with the amplitudes of these components given by a spectral model. The spectral model is characterised by the parameters H_s and T_z . The Pierson Moskowitz spectral model is for a fully developed sea and is given as:

$$S_{pm}(\omega) = \frac{0.11H_s^2T_z}{2\pi} \left(\frac{\omega T_z}{2\pi}\right)^{-5} e^{[-0.44\left(\frac{\omega T_z}{2\pi}\right)^{-4}]}$$
 (11)

A time series corresponding to the surface elevation of a fully developed sea is calculated by dividing this spectrum (for a particular H_s and T_z) into regularly spaced frequency components at intervals of $d\omega = 0.00625$ rad/s up to a maximum frequency of 3.5 rad/s. The surface elevation is then calculated as:

$$\eta(t) = \sum_{i=1}^{512} a(i) \sin(\omega(i)t + \phi(i))$$
 (12)

where

$$a(i) = \sqrt{2E_{\omega}(\omega(i))d\omega}$$
 (13)

where $\phi(i)$ are random phase angles uniformly distributed between 0 and 2π .

Current practice [?] uses a $d\omega$ anywhere between 0.00625 and 0.0325 rad/s. We will now look at the implications that the choice of $d\omega$ has on the realism of the simulated surface elevation time series. Fig. 15 (b) shows the wavelet transform of a simulated surface elevation time series calculated using the above process. Fig. 15 (c) shows the wavelet transform of a simulated surface elevation time series calculated using the same process but with $d\omega = 0.0625$ rad/s. The effect of the increase in $d\omega$ is clearly visible with the time series appearing to repeat approximately every 100 seconds. In this case, measures such as the mean frequency across the wavelet transform (μ_w), the standard deviation of the peak frequency across the wavelet transform (σ_w) and the mean magnitude of the peak frequency have changed significantly from Fig. 15 (b). Fig. 16 illustrates the variation in these wavelet spectrum measures, along with the standard deviation of the magnitude of the peak frequency and the maximum magnitude of the peak frequency, for variations in $d\omega$ when simulating a surface elevation wave time series.

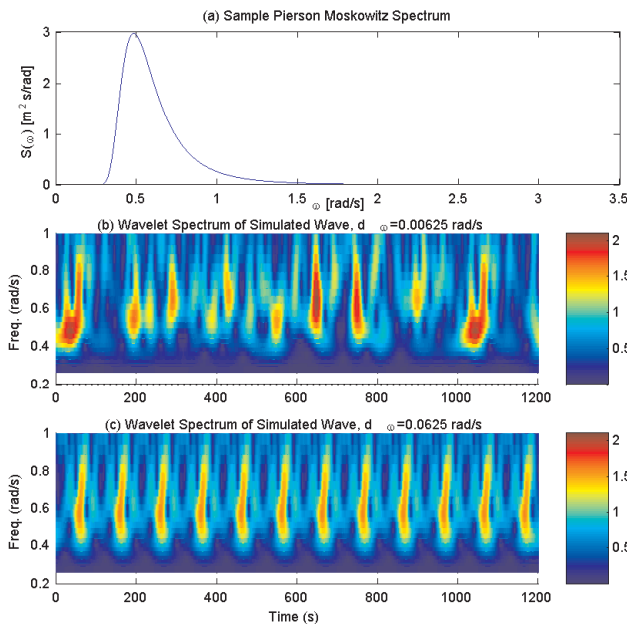


Figure 15: Pierson Moskowitz spectrum and the wavelet transform of two simulated wave records

There exists a clear inverse correlation between $d\omega$ and,

- σ_w (Fig. 16 (b)),
- The standard deviation of the magnitude of the peak frequency (Fig. 16 (d)), and
- The maximum magnitude of the peak frequency (Fig. 16 (e)).

Returning to the measured (off the West Coast of Ireland) wave records, Fig. 17 (a) and (b) show the wave spectrum and the wavelet spectrum calculated from a wave record measured on the 12th of February 2005. Part (c) of the same figure shows the wavelet spectrum of a simulated wave surface elevation time series, where the time series has been created by dividing the wave spectrum of Fig. 17 (a) with intervals of $d\omega = 0.00625$ rad/s and summing the various wave components as in equation (12). Interestingly, the wavelet transforms of part (b) and (c) seem

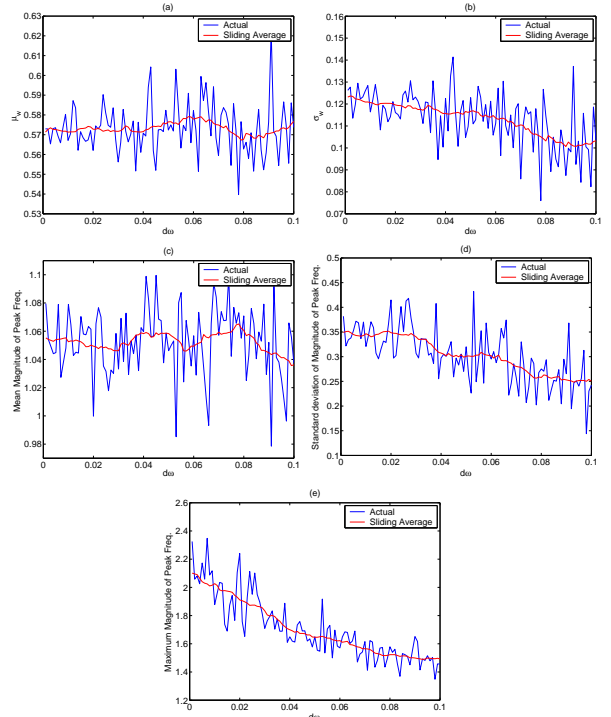


Figure 16: Summary measures of the wavelet transform of simulated wave surface elevation time series with varying $d\omega$

to have similar levels of intermittency in the wave activity. To verify this, Table 2 shows the average summarising measures of 5 wavelet transforms calculated from 5 simulated surface elevation time series calculated from the spectrum of Fig. 17 (a). It can be seen that good agreement exists between the results from the original wave record and the simulated wave record suggesting that $d\omega = 0.00625$ rad/s is an appropriate interval for dividing wave spectra to simulate wave records (this exercise was repeated for a number wave spectra and in each case good agreement, in terms of the wave activity and its intermittency, was found between the original and the simulated wave records).

Time Series	Real	Simulated
μ_w	0.643	0.646
σ_w	0.104	0.115
Mean magnitude of peak freq.	1.453	1.404
Standard deviation of magnitude of peak freq.	0.49	0.557
Maximum magnitude of peak freq.	2.766	2.971

Table 2: Summary statistics of the wavelet transform for the original and simulated wave records

3 Conclusions

This paper has introduced the wavelet spectrum as an effective tool for the analysis of the short term temporal variability of energy in ocean wave surface elevation time records.

The wavelet transform was used to investigate the belief that high energy wave systems (dominated by large swell waves) are more regular, in terms of period or frequency, than wave systems consisting of small swell

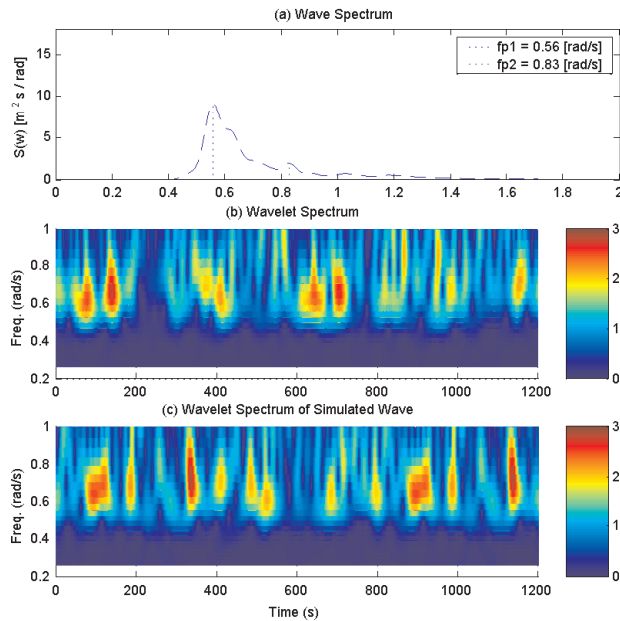


Figure 17: (a) Wave spectrum of a 20 minute wave record, (b) wavelet spectrum of the same record and (c) wavelet spectrum of a simulated wave record from the wave spectrum in (a)

waves with local irregular wind generated waves. However, no direct correlation between energy and regularity could be identified in the wave records measured off the West Coast of Ireland. As expected, an inverse correlation between energy and peak frequency could be clearly identified in the wave records (high energy swell waves with lower frequency than the lower energy higher frequency local wind waves).

The problem (for wave energy device designers) of different spectral shapes with the same H_s and T_z was highlighted. However, it was noted that wave records consisting of two significant wave systems (i.e. two clear peaks in the records wave spectra) contributed most of the occasions when the shape of the wave spectrum of a wave record significantly differed from the classic wave spectral shape. Occurrences of such wave systems was found to be low and mainly during winter months during the occasions when the total energy in the combined wave systems was particularly low.

Finally, the wavelet transform was used to look at the practice of simulating ocean wave surface elevation records from spectral models. It was shown that dividing the wave spectra with an interval of 0.00625 rad/s and summing the components using random phase angles uniformly distributed between 0 and 2π was appropriate to generate realistic ocean wave records. The problem of not dividing the wave spectra into a sufficient amount of components was illustrated.

Acknowledgements

The authors are grateful for the financial support provided by the Irish Marine Institute under the Strategic

RTDI Programme (Grant No. ST\05\08). The authors would also like to acknowledge the developers of the freely available WAFO (Wave Analysis for Fatigue and Oceanography) toolbox for Matlab. The toolbox contains routines for statistical analysis (of which a number were utilised in this study) and simulation of random waves and random loads (does not include routines for the wavelet transform).

References

- [1] J. Falnes. *Ocean Waves and Oscillating Systems*. Cambridge University Press, Cambridge, UK, 2002.
- [2] P. Liu. Is the wind wave frequency spectrum outdated. *Ocean Engineering*, 27:577–588, 2000.
- [3] S.R. Massel. Wavelet analysis for processing ocean surface wave records. *Ocean Engineering*, 28:957–987, 2001.
- [4] I. Daubechies. *Ten Lectures on Wavelets*. Society for Industrial and Applied Mathematics, 1992.
- [5] P.S. Addison. *The Illustrated Wavelet Transform Handbook*. Institute of Physics, 2002.
- [6] M.K. Ochi. *Ocean Waves: The Stochastic Approach*. University Press, Cambridge, 1998.
- [7] W.J. Pierson and L. Moskowitz. A proposed spectral form for fully developed wind seas based on the similarity theory of S. A. Kitaigorodskii. *Journal of Geophysical Research*, 69(24):5181–5190, 1964.
- [8] W.E. Cummings, S.L. Bales, and D.M. Gentile. Hindcasting waves for engineering applications. In *Proc. of the International Symposium on Hydrodynamics in Ocean Engineering*, pages 70–89, Trondheim, Norway, 1981.
- [9] C. Guedes Soares and M.C. Nolasco. Spectral modelling of sea states with multiple wave systems. *Journal of Offshore Mechanics and Arctic Engineering*, pages 278–284, 1992.
- [10] G. Rodriguez and C. Guedes Soares. A criterion for the automatic identification of multimodal sea wave spectra. *Applied Ocean Research*, 21:329–333, 1999.
- [11] G. Rodriguez and C. Guedes Soares. Uncertainty in the estimation of the slope of the high frequency tail of wave spectra. *Applied Ocean Research*, 21:207–213, 1999.
- [12] J. Bendat and Piersol J. *Random Data. Analysis and Measurement Procedures*. New York, Wiley, 1986.
- [13] K. Hasselmann, T.P. Barnett, E. Bouws, H. Carlson, D.E. Cartwright, K. Enke, J.A. Ewing, H. Gienapp, D.E. Hasselmann, P. Kruseman, A. Meerburg, P. Müller, D.J. Olbers, K. Richter, W. Sell,

and H. Walden. Measurements of wind-wave growth and swell decay during the joint north sea wave project (JONSWAP). Technical re-

port, Deutschen Hydrographischen Institut, Hamburg, Germany, 1973.